



Xuelian injection ameliorates complete Freund's adjuvant-induced acute arthritis in rats via inhibiting TLR4 signaling

Li-Shan Yan^{a,1}, Brian Chi-Yan Cheng^{b,1}, Yi-Wei Wang^{a,1}, Shuo-Feng Zhang^a, Xin-Yu Qiu^a, Jian-Ying Kang^a, Chao Zhang^a, Zhan-Hong Jia^a, Gan Luo^{a,*}, Yi Zhang^{a,**}

^a School of Chinese Materia Medica, Beijing University of Chinese Medicine, Beijing 100029, PR China

^b Hong Kong Productivity Council, Hong Kong, PR China

ARTICLE INFO

Keywords:

Xuelian injection
Rheumatoid arthritis
RAW264.7 macrophages
TLR4 signaling pathways

ABSTRACT

Background: Xuelian injection (XI), a classic preparation extracted from *Saussureae Involucratae Herba*, has been clinically used to manage rheumatoid arthritis (RA) for nearly twenty years in China. However, the underlying *anti*-RA mechanism of XI remains unclear. In this study, complete Freund's adjuvant (CFA)-induced acute arthritic model was used to examine the *anti*-RA effects of XI *in vivo*. The molecular mechanisms of this action were further investigated using lipopoly-saccharide (LPS)-stimulated RAW 264.7 macrophages.

Methods: XI and XI freeze dried powder were characterized by UPLC analysis. CD68 and TLR4 expression in the ankle joints was measured by immunohistochemistry. The secretion of inflammatory mediators was detected by ELISA. The expression levels of TLR4 involved components were measured by Western blotting. The localization of transcription factors was measured by immunofluorescence assay.

Results: XI treatment ameliorated arthritic symptoms induced by CFA in the ankle joints of rats. The serum levels of inflammatory mediators, including TNF- α , MCP-1, and Rantes were decreased by XI treatment. The elevation of CD68 and TLR4 levels in ankle joints caused by CFA was suppressed by XI treatment. Moreover, XI treatment inhibited the secretion of nitric oxide and prostaglandin E2 in LPS-treated RAW264.7 macrophages. The expression of their enzymes iNOS and COX-2 was also decreased after XI treatment. The production of inflammatory mediators, including TNF- α , IL-6, IL-1 β , MCP-1, MIP-1 α , and Rantes was reduced by XI treatment in LPS-stimulated RAW264.7 cells. The phosphorylation of p38, JNK, ERK, TBK1, IKK α / β , I κ B, p65, c-Jun, and IRF3 was reduced after XI treatment. Additionally, the expression levels of nuclear proteins of p65, c-Jun, and IRF3 were inhibited by XI treatment.

Conclusions: Taken together, XI possesses potential *anti*-RA effect and the underlying mechanism may be closely associated with the inhibition of TLR4 signaling. Our findings provide further pharmacological justifications for the clinical use of XI in RA treatment.

* Corresponding author.

** Corresponding author.

E-mail addresses: luna049@126.com, 201701032@bucm.edu.cn (G. Luo), yizhang714@163.com, 201601019@bucm.edu.cn (Y. Zhang).

¹ These authors contributed equally to this work.

1. Introduction

Rheumatoid arthritis (RA) is a chronic, progressive, and disabling autoimmune disease that may affect many tissues and organs and primarily cause permanent joint destruction and deformity [1]. RA is prevalent in about 0.46 % of the world population and shortens the lifespans of patients, imposing a huge clinical and economic burden on the society [2,3]. Until now, in addition to methotrexate as a conventional synthetic disease-modifying anti-rheumatic drug, glucocorticoids are used in RA for “bridging” therapy during episodes of high disease activity considering their rapid onset of action and efficacy in relieving pain and stiffness [4]. However, these drug treatment options may not bring satisfactory efficacy because of their serious side effects due to long-term administration [5,6]. Therefore, seeking safety and effective agents is urgently needed for RA treatment.

The pathogenesis of RA is complex and closely related to the inflamed synovial joints which are enriched with activated macrophages [7]. They are the main source of pro-inflammatory cytokines, chemokines, and tissue-destructive enzymes, which cause cartilage and bone erosion in RA patients [8]. Molecular evidences showed that TLR4 signaling affects macrophages which mediate adaptive immune responses [9]. Initiation of TLR4 signaling cascades leads to the activation of three transcription factors, including NF- κ B, AP-1 and IRF3, which in turn promotes the release of inflammatory mediators, such as TNF- α , IL-6, MCP-1 and Rantes, contributing to RA development [10,11]. Therefore, inhibition of the activation of intermediary proteins downstream of TLR4 signaling can mitigate TLR4-triggered inflammatory responses in macrophages and benefit for RA management.

Saussurea involucrata (Kar. et Kir.) Sch.-Bip (Tian-Shan-Xue-Lian in Chinese) is a rare and beneficial traditional Chinese medicinal herb. Xuelian injection (XI), a pharmaceutical product composed of the extract of overground part of *Saussurea involucrata*, is officially used in hospitals in China for treatment of RA for nearly twenty years [12]. Previous studies reported that XI treatment inhibited the production of cerebral TNF- α , IL-1 β , and MMP-9 in ischemia/reperfusion rat model [13]. However, there are few studies issued on the anti-RA property of XI and the underlying mechanism of this action remains unclear. To further provide pharmacological justification for the application of XI in treating RA, in this study, we employed complete Freund's adjuvant (CFA)-induced acute arthritic (AA) rat model to investigate the anti-RA effect of XI. LPS-stimulated RAW264.7 macrophages, a classic inflammatory cell model, was also used to explore the underlying molecular mechanism.

2. Materials and methods

2.1. Reagents

CFA, modified Griess reagent, 3-[4,5-dimethylthiazol-2-yl]-2,5-diphenyl tetrazolium bromide (MTT), lipopolysaccharide (LPS, *Escherichia coli* O55:B5) were purchased from Sigma Chemical Co. (St. Louis MO, USA). Dulbecco's Modified Eagle Medium (DMEM) was acquired from Corning Cellgro (Manassas, VA, USA). Penicillin-streptomycin solution was obtained from Caisson labs (Smithfield, UT, USA). Fetal bovine serum (FBS) was bought from Biological Industries Co. (Beth-Haemek, Israel). Dexamethasone sodium phosphate injection was bought from Tianjin Jinyao Pharmaceutical Co Ltd. (Lot number: 2004232, China). Tumor necrosis factor α (TNF- α , cat. # 88-7324-22 and 88-7340-22 for mouse and rat, respectively), interleukin 6 (IL-6, cat. # 88-7064-22), interleukin 1 β (IL-1 β , cat. # 88-7013-22), macrophage inflammatory protein 1 α (MIP-1 α , cat. # 88-56013-22), monocyte chemoattractant protein 1 (MCP-1, cat. # 88-7391-22 and BMS631INST for mouse and rat, respectively), and regulated upon activation normal T cell expressed and secreted factor (Rantes, cat. # KMC1031 and KRC1031 for mouse and rat, respectively) ELISA kits were purchased from Thermo Fisher Scientific (San Diego, CA). Prostaglandin E2 (PGE2) ELISA kit (cat. # ADI-900-001) was provided by Enzo Life Sciences (Exeter, UK). Antibody against CD68 (cat. # sc-20060) was supplied by Santa Cruz Biotechnology (CA, USA). Anti- $\text{IKK}\beta$ (cat. # 15649-1-AP) and Sp1 (cat. # 21962-1-AP) antibodies were from Proteintech (Rosemont, USA). Anti-interferon regulatory factor 3 (IRF3, cat. # ab68481) and anti-inducible nitric oxide synthase (iNOS, cat. # ab3523) antibodies were purchased from Abcam (Cambridge, UK). Anti-phospho-IRF3 (Ser396, cat. # PAB31634) antibody was provided by ABNOVA (Taiwan, China). Antibodies against phospho-NF- κ B p65 (Ser536, cat. # 3033), NF- κ B p65 (cat. # 8242), phospho-c-Jun (Ser73, cat. # 9164), c-Jun (cat. # 9165), cyclooxygenase-2 (COX-2, cat. # 12282), phospho-I κ B α (Ser32, cat. # 2859), I κ B α (cat. # 4812), phospho- $\text{IKK}\alpha/\beta$ (Ser176/177, cat. # 2078), extracellular signal-regulated kinase (ERK, cat. # 4695), phospho-ERK (Thr202/Tyr204, cat. # 4370), c-Jun N-terminal kinase (JNK, cat. # 9252), phospho-JNK (Thr183/Tyr185, cat. # 4668), p38 mitogen-activated protein kinase (p38, cat. # 8690), phospho-p38 (Thr180/Tyr182, cat. # 4511), TANK-binding kinase 1 (TBK1, cat. # 3013), phospho-TBK1 (Ser172, cat. # 5483), β -actin (cat. # 4970), anti-rabbit IgG HRP linked antibody (cat. # 7074), and Alexa Fluor 488-conjugated secondary antibody (cat. # 4412) were bought from Cell Signaling Technology (Boston, MA, USA). Antibody against TLR4 was obtained from Wuhan Servicebio Technology Co., Ltd. (cat. # Gb12186, Wuhan, China). Chlorogenic acid (Lot number: A22GB158496) was purchased from Shanghai Yuanye biotechnology Co., Ltd. (Shanghai, China). Rutin (Lot number: 100080-201811) was obtained from National Institutes for Food and Drug Control (Beijing, China). Acetonitrile was obtained from Thermo Fisher Scientific (Waltham, Massachusetts, USA).

2.2. Preparation and characterization of XI and XI freeze dried powder

XI (Lot number: 180703) was bought from Sinopharm Xinjiang pharmaceutical Co., Ltd. XI was concentrated by rotary evaporation under reduced pressure to remove the solvent. The concentrated extracts were rapidly frozen at -80°C , and then dried in a freeze-dryer (FD-1D-80, Biocool, Beijing, China) to produce freeze dried powder. XI was shaken and filtered through a Millipore membrane filter with an average pore diameter of 0.22 μm for UPLC analysis. To characterize the XI freeze dried powder, 0.0589 g powder was dissolved in 50 % methanol and diluted to a final volume of 10 mL. After being filtered through a 0.22 μm pore-size membrane

filter, the subsequent filtrate was used for UPLC analysis. The contents of chlorogenic acid and rutin in XI and XI powder were quantitated by an Acquity UPLC system (Waters, Milford, Massachusetts, USA). The separation was performed on an ACQUITY UPLC®HSS T3 column (1.8 μm , 100 mm \times 2.1 mm) with a Van Guard™ Pre-Column (1.8 μm). The gradient mobile phase was consisted of solvent A (acetonitrile) and solvent B (0.1 % formic acid in water). The UPLC elution profile was set as follows: 5–9% A for 0–6 min, 9–13 % A for 6–12 min, 13–16 % A for 12–19 min, 16–17 % A for 19–28 min, 17–28 % A for 28–40 min. The flow rate was maintained at 0.3 mL·min⁻¹ and the column temperature was set at 30 °C. The chromatograms were monitored with the variable wavelength detector at wavelength of 340 nm to detect chlorogenic acid and rutin.

2.3. Animal treatments

Male Sprague-Dawley rats (Grade SPF), weighing 180–220 g, were purchased from Beijing Sabei Fu Biotechnology Co., Ltd. (Beijing, China; certificate no. SCXK [jing] 2019–0010). The animals were maintained in the animal facility at the Department of Pharmacology, School of Chinese Materia Medica, Beijing University of Chinese Medicine. All the animal studies were in accordance with ethics standards of the Animal Care and Welfare Committee of Beijing University of Chinese Medicine [Certificate No. BUCM-4-2021110803-4040]. Rats were maintained at 22–23 °C with a relative humidity of 50–55 % and had free access to water and food. Rats were randomly divided into 6 groups of 10 animals in each, including control, model, positive control drug (dexamethasone, Dex, 0.5 mg/kg), XI (low dose, 0.45 mL/kg), XI (medium dose, 0.9 mL/kg) and XI (high dose, 1.8 mL/kg) groups. In each group, 5 rats were housed in one cage. On the 1st day, 0.1 mL CFA was injected intradermally into the left hind paw of each rat except rats in the control group. The rats in the control group were injected with the same amount of saline. On the 7th day, the rats (except the control rats) were received a booster injection of 0.1 mL CFA and were then once daily intraperitoneally treated with XI at doses of 0.45, 0.9, and 1.8 mL/kg or 0.5 mg/kg dexamethasone or saline (0.9 mL/kg), respectively. Rats in control group were treated with saline (0.9 mL/kg). After 13-day treatment, rats were fasted for 12 h (from 00:00 to 12:00). The hind paw volume was determined with a water displacement plethysmometer (YLS-7B; Yiyang Technology Co, Jinan, China) and the perimeter of hind paw was also measured. The swelling ratio of hind paw volume/perimeter was calculated as (%)=(left hind paw-right hind paw)/right hind paw \times 100 %. The blood and left hind paws were obtained from pentobarbital sodium-anesthetized animals. Serum samples were prepared by centrifuging the whole blood collected from the orbital vein for 15 min at 2000 \times g and 4 °C, and then stored at –80 °C until use.

2.4. Hematoxylin and eosin staining

The left ankle joints were fixed in 10 % neutral formalin solution for 72 h, and then washed with distilled water and decalcified with EDTA decalcification fluid (G1105, Wuhan Servicebio Technology, China). The tissue samples were embedded in paraffin and cut into 4 μm thick slices. The sections were stained with hematoxylin and eosin (H&E) and observed under Nikon Eclipse 80i microscope (Tokyo, Japan) by an observer that was blinded to the experimental design to identify the presence of (1) inflammatory cell infiltration, (2) synovial hyperplasia/pannus formation, (3) bone erosions, and (4) cartilage destruction. The severity of acute arthritis was assessed by summaries of the four lesion scores ranging from 0 to 3 [14].

2.5. Immunohistochemical analysis of the ankle joints

Immunohistochemical staining was performed by Servicebio Technology Co., Ltd (Wuhan, China). Briefly, the paraffin sections of left ankle joints were deparaffinized and rehydrated. The antigen was heat-repaired with citric acid for 45 min. Subsequently, the sections were blocked with hydrogen peroxide solution (3 %) for 25 min and washed with PBS for 3 times. The slides were then blocked by BSA (3 %) for 30 min at room temperature (RT) and incubated with primary antibody against CD68 or TLR4 overnight at 4 °C. After washing three times with PBS, the slides were incubated with HRP goat anti-mouse IgG secondary antibody (GB23301, Wuhan Servicebio Technology, China) for 50 min at RT. Next, the slides were stained with DAB color developing solution (G1212, Wuhan Servicebio Technology, China) for about 25 min and washed with distilled water for 3 times. The slides were then counterstained with hematoxylin for 3 min, dehydrated and mounted. Images were taken using a Nikon Eclipse 80i microscope. For quantitative analysis of the expression levels of CD68 and TLR4, the positive staining area of each image was measured by Image-Pro Plus 5.1 (Media Cybernetics, Rockville, MD, USA). Three images for each slice were analyzed. 5–6 animals for each group were used.

2.6. Cell culture

RAW264.7 cells (kindly provided by Prof. Zhi-Xiang Zhu, Beijing University of Chinese Medicine, China) were maintained in DMEM supplemented with 100 U/mL penicillin, 100 $\mu\text{g}/\text{mL}$ streptomycin and 10 % fetal bovine serum in a CO₂ incubator (Thermo fisher scientific, under a humidified atmosphere of 5 % CO₂ and 95 % air) at 37 °C. XI freeze dried powder was accurately weighted and dissolved in PBS to prepare the stock solution.

2.7. Cell viability assay

RAW264.7 cells were seeded (6 \times 10³ cells/well) and cultured in 96-well plates for 24 h. The cells were then treated with LPS (1 $\mu\text{g}/\text{mL}$) and various concentrations of XI (6.25–400 $\mu\text{g}/\text{mL}$) for 24 h at 37 °C. Cells were incubated at 37 °C with 10 μL MTT solution (5 mg/mL) in each well for 3 h. The supernatant was removed and the remaining formazan crystals were dissolved with 100 μL DMSO in

each well. Absorbance was detected at 570 nm by using a SPECTROstar Nano microplate reader. The results were compared with the cell viability in the control group. Six replicate wells were conducted for each group.

2.8. Detection of inflammatory mediators

Cytokine and chemokine levels in the culture medium or serum were quantified by ELISA kits. Briefly, RAW264.7 cells were seeded into 24 well plates (2×10^5 cells/well) overnight. The cells were pre-treated with XI (50–400 $\mu\text{g}/\text{mL}$) for 1 h and then treated with or without LPS (1 $\mu\text{g}/\text{mL}$) for 24 h. The culture medium was obtained for the determination of PGE2, IL-6, TNF- α , IL-1 β , MCP-1, MIP-1 α , and Rantes using ELISA kits following the manufacturer's instructions. Levels of nitric oxide (NO) in the culture medium were determined by Griess assay. Four replicate wells were used for each group. The contents of TNF- α , MCP-1, and Rantes in serum were detected by using ELISA kits according to the manufacturer's protocols. Ten serum samples for each group were used.

2.9. Western blotting

The expression levels of proteins were assessed by Western blotting analysis. Briefly, cells (5×10^5) were seeded into 60 mm culture dishes, and then treated with XI at two concentrations (200 and 400 $\mu\text{g}/\text{mL}$). LPS (1 $\mu\text{g}/\text{mL}$) was added 1 h after XI pre-treatment, and the cells were incubated at 37 °C for 30 or 60 min. The cells were lysed with RIPA buffer (Beyotime biotechnology, Beijing, China) or extracted by using nuclear extraction kit (Solarbio, Beijing, China) following the manufacturer's protocols. A small aliquot (40 μg) of the supernatant protein from each sample was heated with sodium dodecyl sulfate (SDS) sample buffer (Lablead, Beijing, China) at 95 °C for 8 min. Protein samples were subjected to SDS-PAGE and then transferred onto polyvinylidene fluoride membrane. The membrane was blocked with 5 % non-fat milk in TBST and incubated with primary antibodies at 4 °C for 12 h. The membrane was then washed with TBST for three times and incubated with anti-mouse or anti-rabbit secondary antibody. The immunoreactive protein bands were detected using enhanced chemiluminescence detection kit (Tanon, Shanghai, China) following the manufacturer's

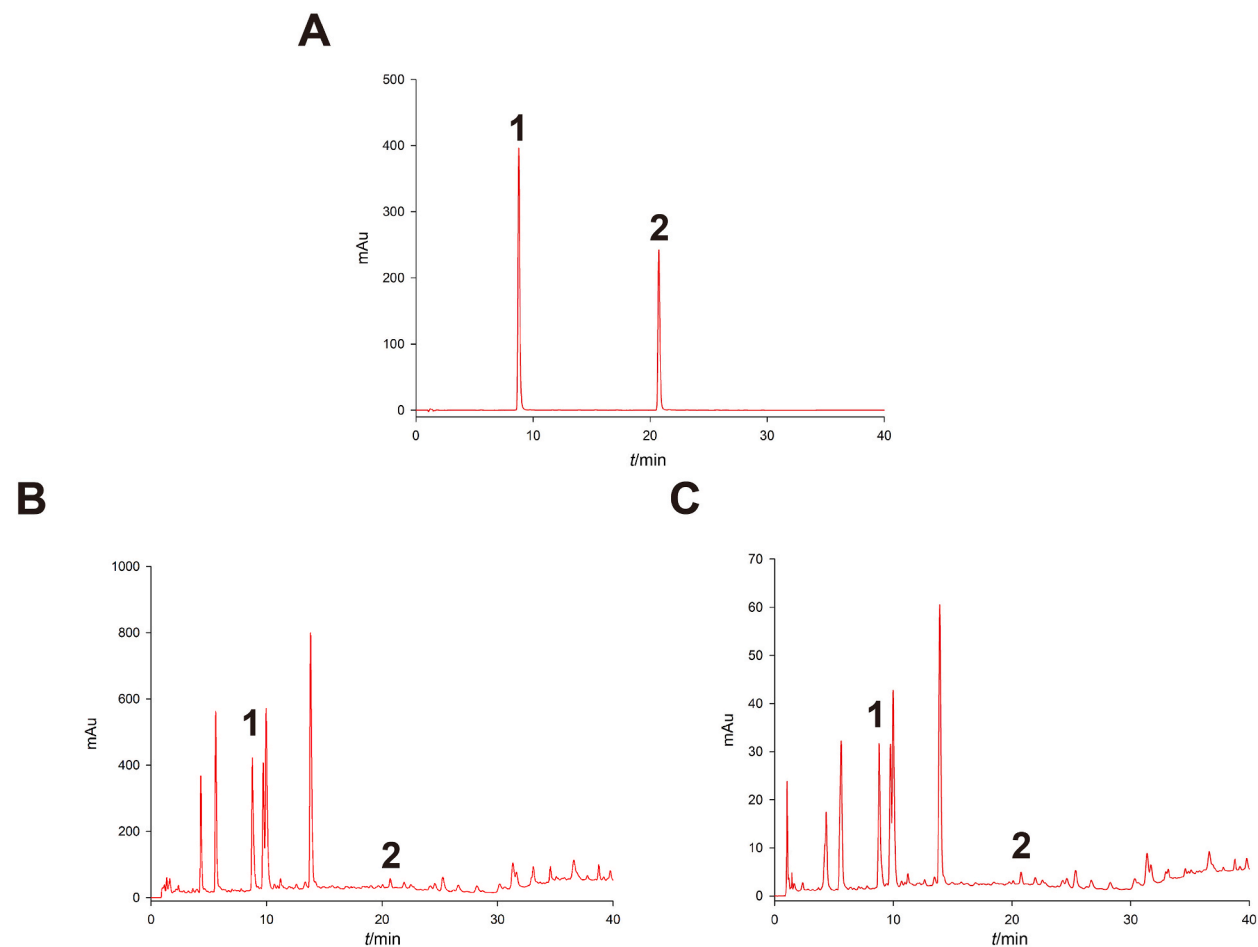


Fig. 1. Characterization of XI and XI freeze dried powder. UPLC chromatogram of chlorogenic acid and rutin (A), XI (B) and XI freeze dried powder (C). Peak 1 and 2 represent chlorogenic acid and rutin, respectively.

instruction. The expression of each protein was quantified using the ImageJ software (National Institutes of Health [NIH], Bethesda, MD, USA). The expression levels of protein were normalized to the matching densitometric value of the internal control β -actin/Sp1. Three replicates were conducted for each group.

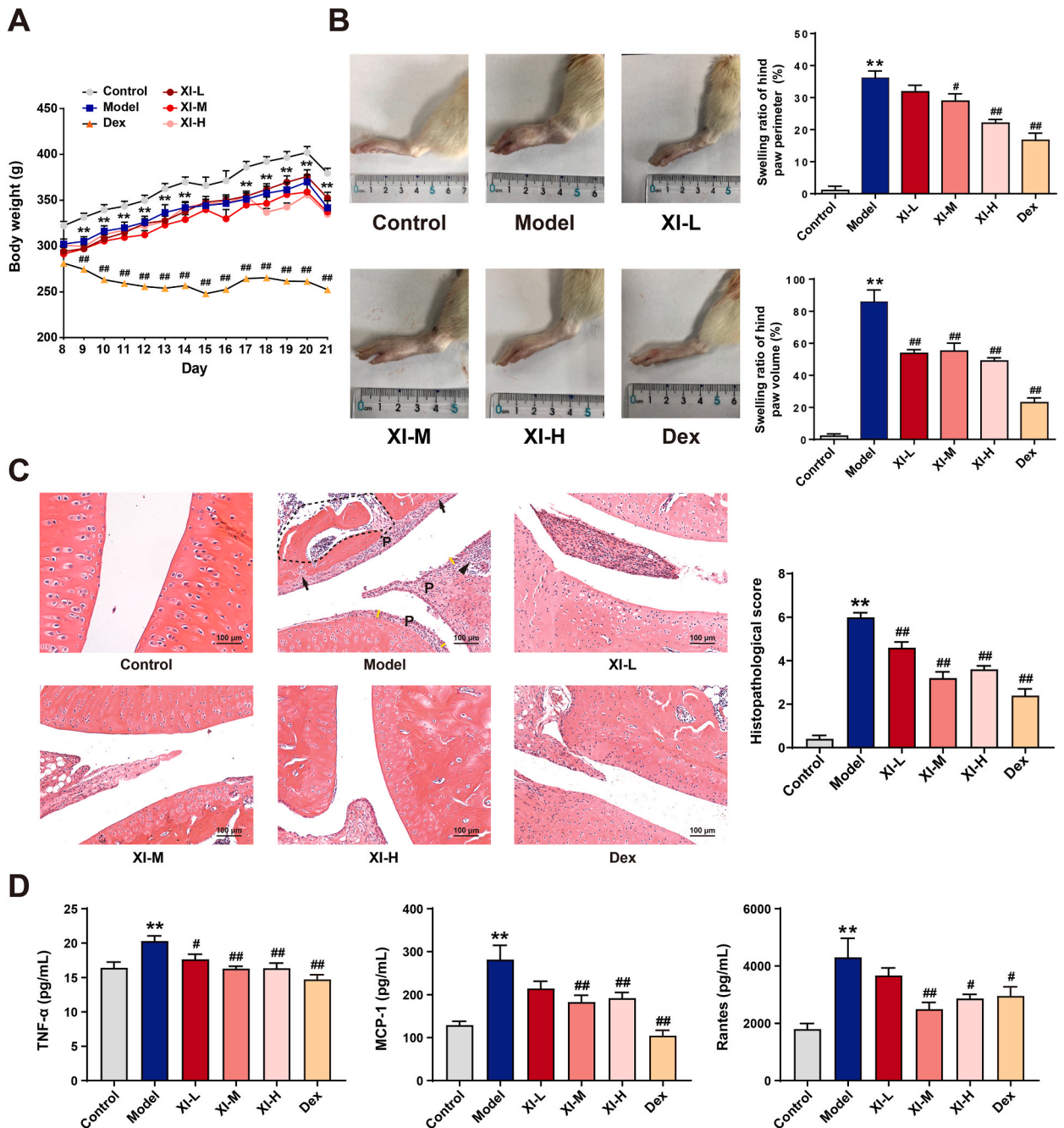


Fig. 2. Effect of XI on clinical arthritic conditions and serum inflammatory mediators in AA rats. CFA (0.1 mL) was injected intradermally into the left hind paw of each rat on day 1 and 7, respectively. Rats were intraperitoneally injected with XI (0.45, 0.9, and 1.8 mL/kg) or Dex (0.5 mg/kg) for 13 days. Rats were then sacrificed, and serum and left hind paws were obtained. (A) The changes of body weight ($n = 10$). (B) Representative morphological images of left hind paw and changes in swelling ratio of hind paw volume/perimeter ($n = 10$). (C) Representative microscopic images of H&E staining. Histopathological scores were estimated based upon cellular infiltration (arrowhead), synovial hyperplasia (yellow lines showing thickening of synovial lining)/pannus formation (P), subchondral bone erosion (black dash lines) and cartilage destruction (arrows) ($n = 10$). (D) The release of cytokine (TNF- α) and chemokines (MCP-1 and Rantes) in the serum was detected by ELISA ($n = 10$). Data are presented as the mean \pm SEM. Statistical differences were compared using one-way ANOVA followed by Dunnett's post hoc test. ** $p < 0.01$, versus control; # $p < 0.05$ and ## $p < 0.01$, versus model.

2.10. Immunofluorescence staining

Immunofluorescence staining was performed to detect NF- κ B, AP-1, and IRF3 localization after XI treatment as previously described [15]. Briefly, cells (1×10^4) were seeded into chamber slide for 12 h, and then pretreated with XI (200 and 400 μ g/mL) for 1 h. The cells were then treated with LPS (1 μ g/mL) for 1 h, and fixed with formaldehyde in PBS (w:v, 4 %) for 15 min and washed with PBS and permeabilized with Triton X-100 (0.25 %) for 30 min at 37 °C. Cells were then blocked for 30 min with BSA (2 %) at RT and incubated with p65 (1:300), c-Jun (1:300), and IRF3 (1:100) overnight at 4 °C, followed by subsequent PBS rinses. Then, cells were incubated with fluorescence-labeled goat anti-rabbit secondary antibody (1:500) at RT without exposure to light for 1 h. PBS washing was repeated, and the nucleus was stained with DAPI fluoromount-GTM (YESEN, Shanghai, China) and then photographed under a PerkinElmer Ultraview VoX spinning disc confocal microscope (Waltham, MA, USA).

2.11. Statistical analysis

All values are expressed as means \pm standard error of mean (SEM). Data were analyzed by one-way ANOVA using GraphPad Prism (version 9.0.0; GraphPad Software, San Diego, CA, USA), and the differences among means were analyzed using Dunnett's multiple comparison test. A difference was considered to be significant when $p < 0.05$.

3. Results

3.1. UPLC determination of chlorogenic acid and rutin in XI and XI freeze dried powder

UPLC analysis showed that chlorogenic acid and rutin were present in XI and XI freeze dried powder (Fig. 1A–C). The contents of chlorogenic acid and rutin in XI and XI freeze dried powder were 62.44/15.15 μ g/mL and 0.09%/0.021 %, respectively.

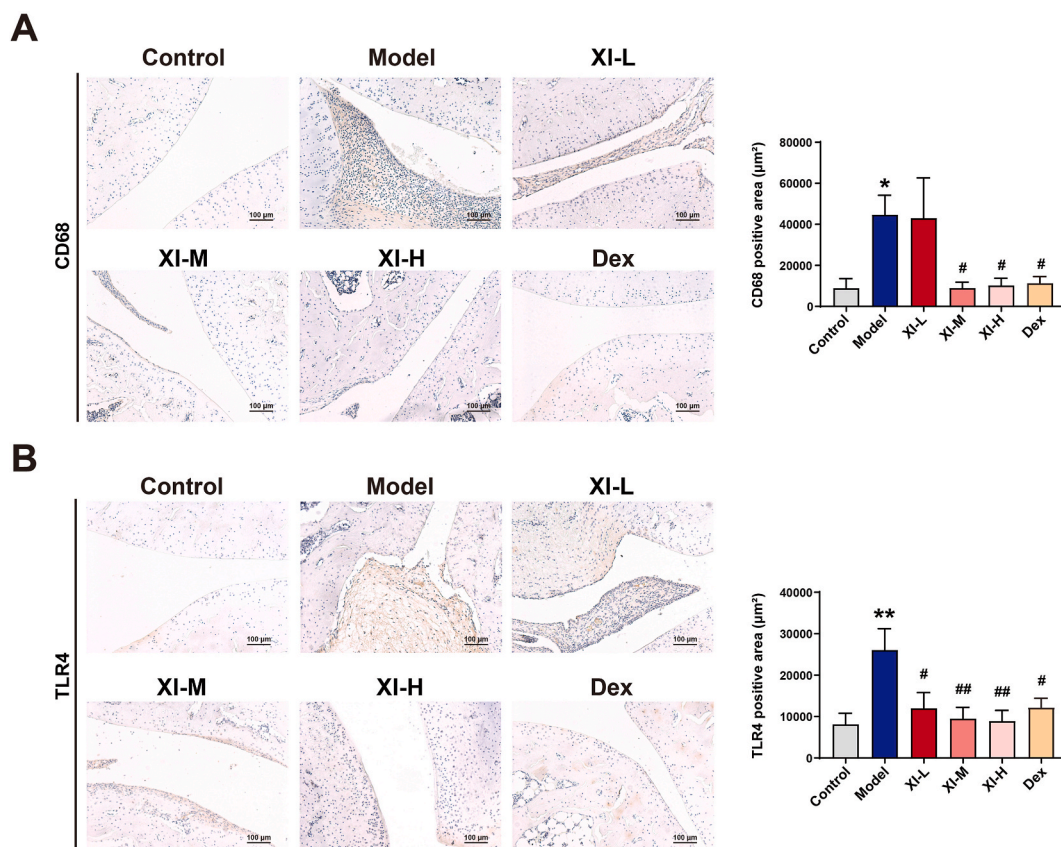


Fig. 3. Effect of XI on CD68 and TLR4 expression in AA rats. Experimental details were as described in Fig. 2. (A) Representative microscopic images of immunohistochemical staining and the positive staining area of CD68 ($n = 5-6$). (B) Representative microscopic images of immunohistochemical staining and the positive staining area of TLR4 ($n = 5-6$). Data presented in bar charts are mean \pm SEM values. Statistical differences were compared using one-way ANOVA followed by Dunnett's post hoc test. * $p < 0.05$ and ** $p < 0.01$, versus control; # $p < 0.05$ and ## $p < 0.01$, versus model.

3.2. XI improved arthritic conditions and inhibited inflammatory mediator production in AA rats

We employed CFA-induced AA rats to assess the *anti*-RA effect of XI. As shown in Fig. 2A, a significant weight loss was observed after Dex treatment. When comparing with model group, no observable weight loss was found in XI-treated groups during the entire experimental period. Representative photographs indicated that the hind paw swelling was significantly elevated after CFA treatment, and XI treatment dose-dependently ameliorated the hind paw swelling, as evidenced by reduction in the swelling ratios of hind paw volume and perimeter (Fig. 2B). The similar observation was found in Dex-treated AA rats. To determine whether XI treatment prevented articular destruction, ankle joints were analyzed histologically. Histopathological examinations showed infiltration of

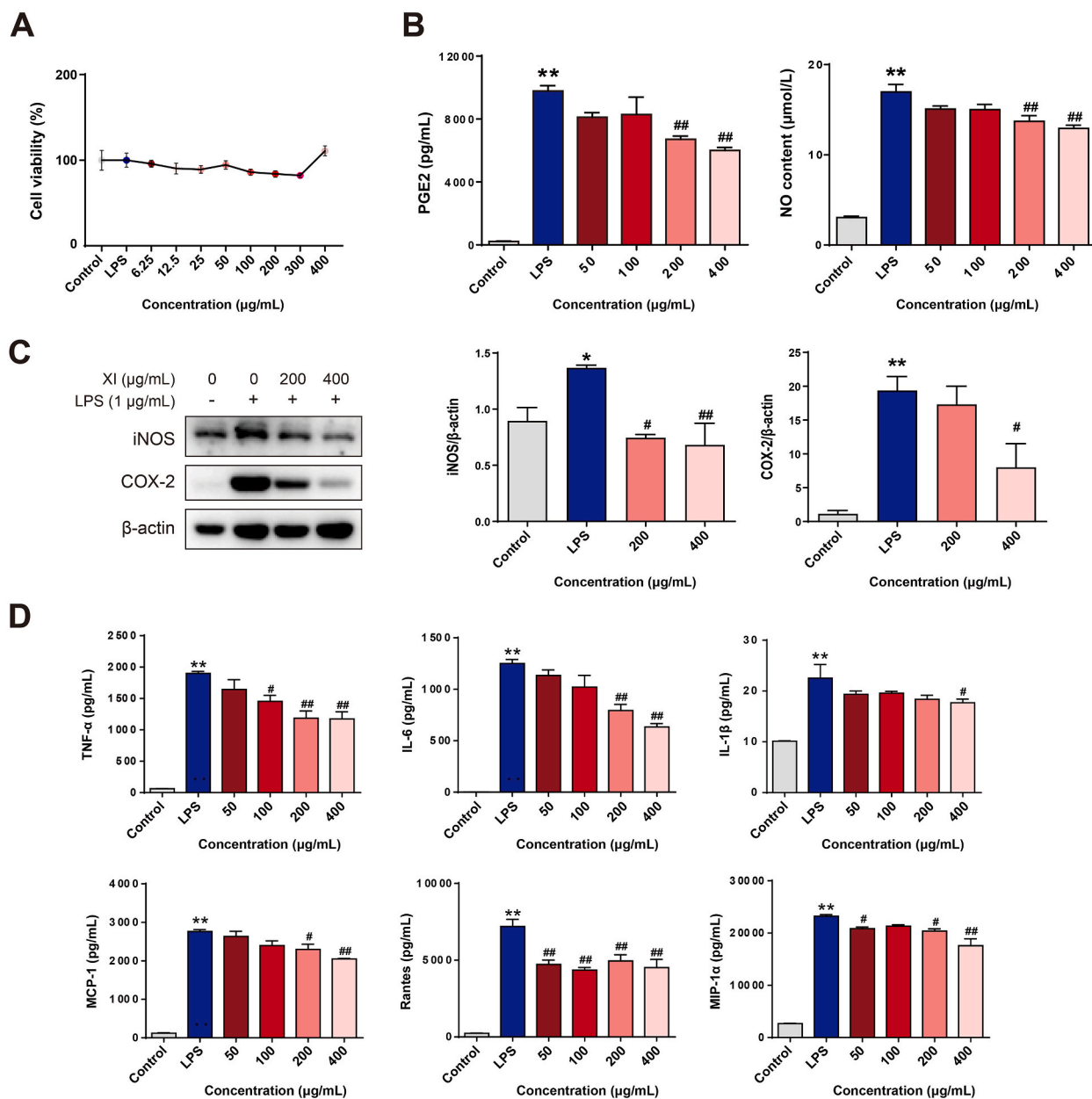
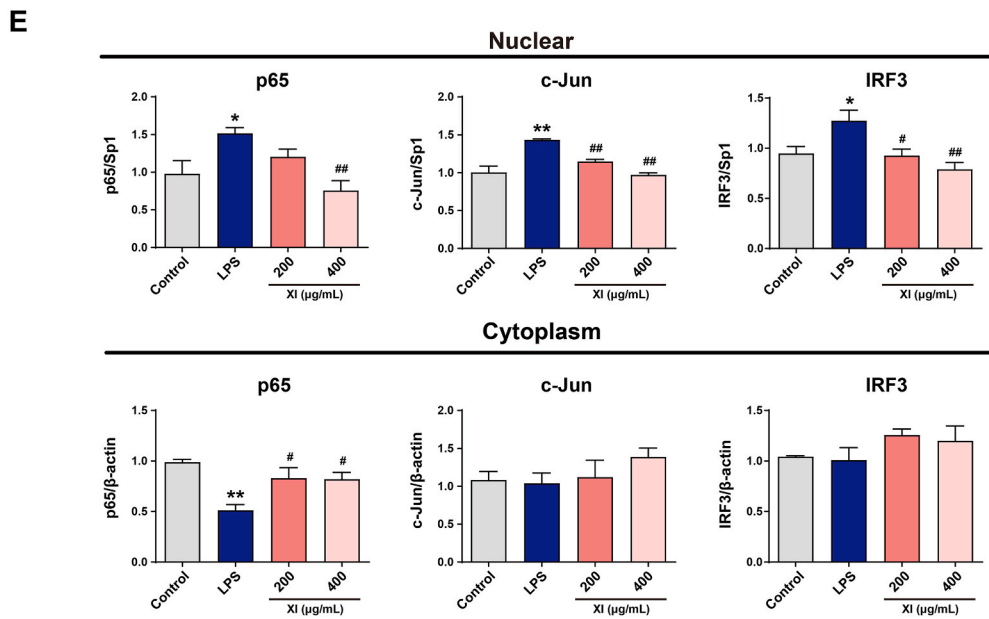
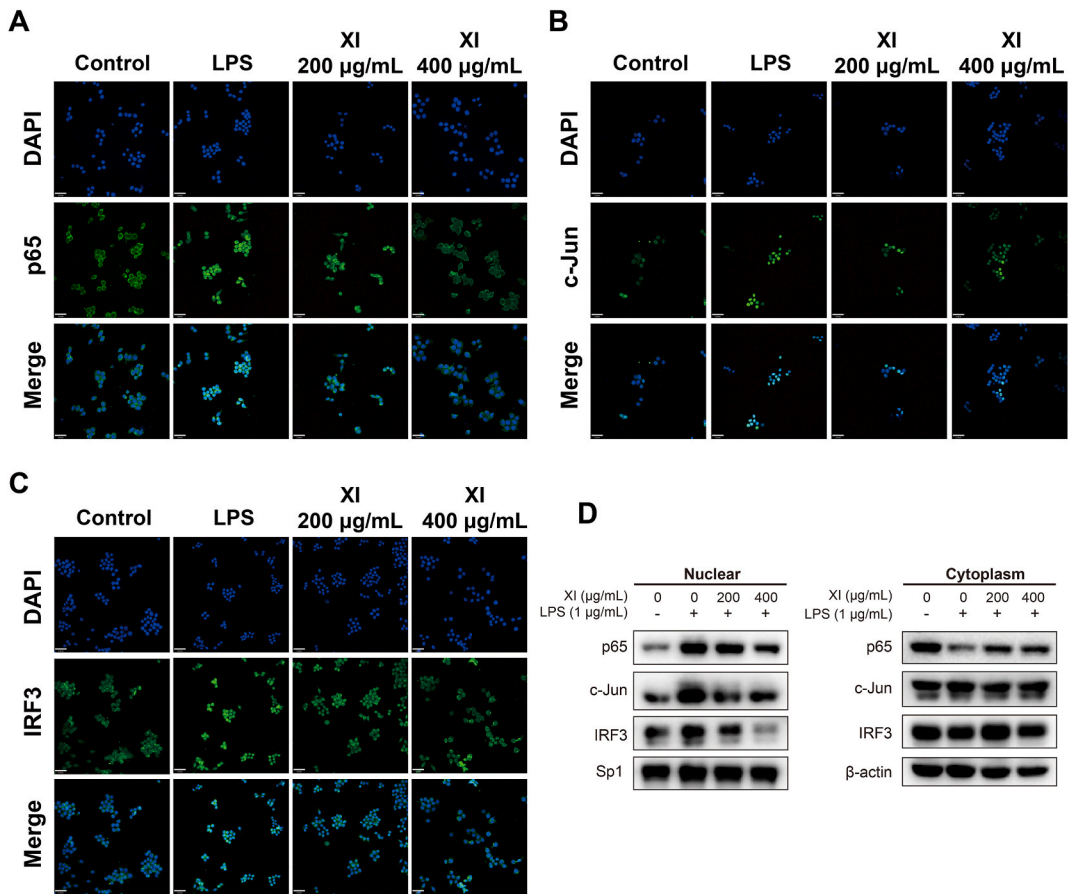


Fig. 4. Effect of XI on the secretion of inflammatory mediators in LPS stimulated RAW264.7 cells. Cells were treated with XI (6.25–400 μg/mL) for 1 h and then stimulated with LPS for 24 h. (A) Cell viability was determined by MTT assay ($n = 6$). (B) The production of NO and PGE2 was detected by Griess reagent and ELISA, respectively ($n = 4$). (C) The protein levels of iNOS and COX-2 were detected by Western blotting ($n = 3$). The original blot images were provided in the Supplementary Material. (D) The release of inflammatory mediators, including TNF- α , IL-6, IL-1 β , MCP-1, MIP-1 α , and Rantes in the culture medium was detected by ELISA ($n = 4$). Data presented in bar charts are mean \pm SEM values. Statistical differences were compared using one-way ANOVA followed by Dunnett's post hoc test. ** $p < 0.01$, versus control; # $p < 0.05$ and ## $p < 0.01$, versus LPS.



(caption on next page)

Fig. 5. Effect of XI on the nuclear translocation of p65, c-Jun, and IRF3 in LPS-stimulated RAW264.7 cells. Cells were pre-treated with XI (200 and 400 $\mu\text{g}/\text{mL}$) for 1 h and then stimulated with LPS for 60 min. (A) The localization of NF- κB , c-Jun and IRF3 was detected using immunofluorescence assay, and the images were acquired using the laser confocal fluorescence microscopy. (B) The expression of nuclear and cytoplasmic proteins was detected by Western blotting ($n = 3$). The original blot images were provided in the Supplementary Material. Data are presented as mean \pm SEM. Statistical differences were compared using one-way ANOVA followed by Dunnett's post hoc test. * $p < 0.05$ and ** $p < 0.01$, versus control; # $p < 0.05$ and ## $p < 0.01$, versus LPS.

inflammatory cells, synovial hyperplasia, pannus formation, and bone erosion were observed in AA rats. XI treatment ameliorated the histopathological changes caused by CFA, which was further confirmed by histopathological scores (Fig. 2C). Moreover, CFA treatment significantly up-regulated the levels of pro-inflammatory mediators, including TNF- α , MCP-1, and Rantes in serum, and XI dose-dependently lowered the levels of these inflammatory mediators (Fig. 2D). Dex treatment also suppressed the production of these three inflammatory mediators in serum.

3.3. XI treatment suppressed the expression of CD68 and TLR4 in AA rats

CD68, which is a heavily glycosylated glycoprotein that is highly expressed in macrophages [16], was detected to evaluate the role of macrophages in the anti-RA effect of XI. Fig. 3A showed that the elevation of CD68 expression in the ankle joint induced by CFA was suppressed by XI treatment. Furthermore, the expression of TLR4 was increased after CFA treatment in the ankle joint, and XI markedly suppressed the expression of TLR4 in a dose-dependent manner (Fig. 3B). These results suggested that XI has the potential to inhibit the activation of macrophages and hinder TLR4 signaling, which may be one of the mechanisms for the anti-RA effects of XI.

3.4. XI treatment inhibited the production of inflammatory mediators in LPS-stimulated RAW264.7 cells

Pro-inflammatory mediators, such as NO and PGE2, were expressed highly in activated macrophages [17,18]. In our present study, exposure of RAW264.7 cells to LPS significantly elevated the production of NO and PGE2, and the enhanced levels of NO and PGE2 were concentration-dependently down-regulated by XI treatment (Fig. 4B). Moreover, the expression of the key enzymes for the NO and PGE2 synthesis, including iNOS and COX-2, was also markedly suppressed by XI treatment (Fig. 4C). XI treatment also decreased LPS-induced secretion of cytokines (IL-6, IL-1 β , and TNF- α) and chemokines (MCP-1, MIP-1 α , and Rantes) in a concentration dependent manner (Fig. 4D). Additionally, MTT assay results indicated that the inhibitory effect of these inflammatory mediators by XI treatment was not caused by its cytotoxicity, because XI at the concentration up to 400 $\mu\text{g}/\text{mL}$ showed no obvious effect on cell viability (Fig. 4A).

3.5. XI treatment hindered the nuclear translocation of NF- κB , AP-1, and IRF3 in LPS-stimulated RAW264.7 cells

Following LPS challenge, NF- κB , AP-1, and IRF3 translocate into the nucleus and activate the transcription of their target genes, promoting inflammatory responses in macrophages [19]. Fig. 5A–C showed that p65, c-Jun, and IRF3 translocated from cytoplasm into the nucleus after LPS exposure. XI treatment concentration-dependently inhibited the nuclear translocation of p65, c-Jun, and IRF3 triggered by LPS treatment. Furthermore, LPS treatment elevated the nuclear protein levels of NF- κB /p65, AP-1/c-Jun, and IRF3, and XI treatment decreased the nuclear protein levels of these three transcription factors. XI also markedly alleviated LPS-induced reduction of cytoplasmic p65. The cytoplasmic proteins of c-Jun and IRF3 were not changed after XI treatment (Fig. 5D and E).

3.6. XI treatment blocked the TLR4 signaling pathways in LPS-stimulated RAW264.7 cells

To understand the molecular mechanism of XI on the inhibition of inflammatory mediators, we further investigated the effect of XI treatment on the TLR4 signaling pathways. Fig. 6 showed that exposure of RAW264.7 cells to 1 $\mu\text{g}/\text{mL}$ LPS elevated the phosphorylation of IKK α/β , I $\kappa\text{B}\alpha$, and TBK1 and these effects were significantly prevented by XI pre-treatment in a concentration-dependent manner. Moreover, LPS stimulation markedly activated the MAPKs, which involve ERK, p38 and JNK in RAW264.7 cells. XI treatment inhibited the phosphorylation of these proteins in a concentration-dependent manner. Moreover, the phosphorylation of p65, c-Jun, and IRF3 was significantly increased after LPS challenge, whereas XI treatment concentration-dependently reduced the phosphorylation of these three proteins (Fig. 6).

4. Discussion

In our study, we found that chlorogenic acid and rutin were present in XI by using UPLC analysis. One study reported that chlorogenic acid has the potential to inhibit collagen-induced arthritis by modulating the activation of the NF- κB signaling pathway [20]. It also effectively ameliorated adjuvant-induced RA in rats via regulating Th1/Th2 balance [21]. In addition, rutin exerted strong ability to protect against RA due to its antioxidant and anti-inflammatory activities [22]. The underlying mechanism of this action may be associated with the inhibitory effect on NF- κB signaling [23]. Thus, chlorogenic acid and rutin may be the material basis for the anti-RA effect of XI.

RA, a chronic and progressive autoimmune disease, is characterized by the interactions of various proinflammatory cytokines and

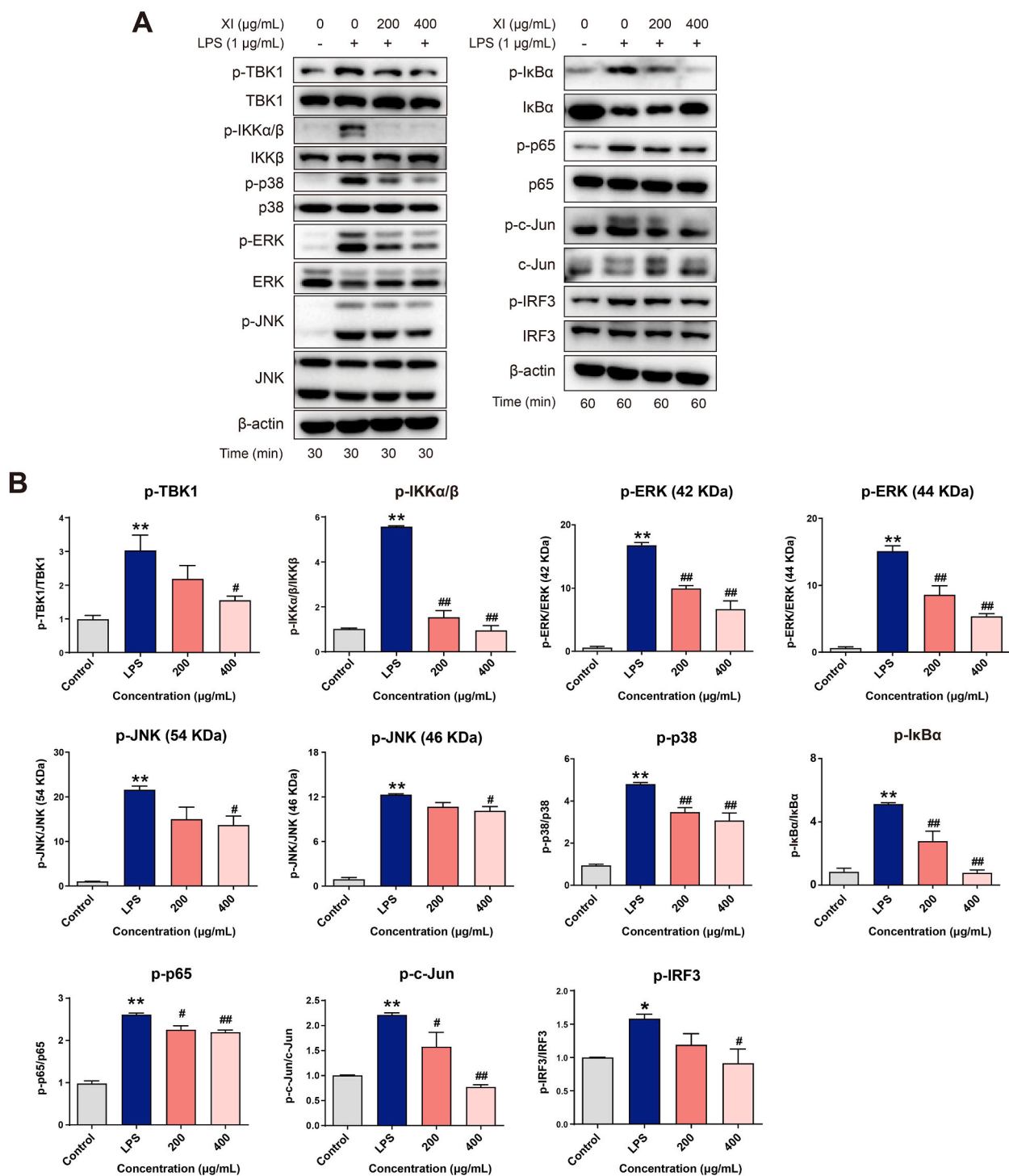


Fig. 6. Effect of XI on TLR4 signaling in LPS-stimulated RAW264.7 cells. Cells were pre-treated with XI (200 and 400 $\mu\text{g/mL}$) for 1 h and then stimulated with LPS for 30 min or 60 min. (A) Levels of p-IKK α/β , IKK β , p-I κ B α , I κ B α , p-p65, p65, p-ERK, ERK, p-JNK, JNK, p-p38, p38, p-c-Jun, c-Jun, p-TBK1, TBK1, p-IRF3, and IRF3 were measured by Western blotting. The original blot images were provided in the Supplementary Material. (B) Bar graphs represent the ratio of p-IKK α/β /IKK β , p-I κ B α /I κ B α , p-p65/p65, p-ERK/ERK, p-JNK/JNK, p-p38/p38, p-c-Jun/c-Jun, p-TBK1/TBK1, and p-IRF3/IRF3 ($n = 3$). Data are presented as the mean \pm SEM. Statistical differences were compared using one-way ANOVA followed by Dunnett's post hoc test. * $p < 0.05$ and ** $p < 0.01$, versus control; # $p < 0.05$ and ## $p < 0.01$, versus LPS.

chemokines released by various immune cells, especially macrophages [24]. Therefore, inhibition of the production of inflammatory mediators released by macrophages is believed to be one of the novel therapeutic approaches in RA management [25,26]. In our present study, XI was found to mitigate the hind paw swelling and inhibit the secretion of cytokines and chemokines caused by CFA without observable adverse effects, suggesting that XI is a potential safe and effective *anti*-RA traditional Chinese medicinal preparation. Besides, histopathological investigations of ankle joints also confirmed the *anti*-RA effects of XI, which were consistent with the results of its inhibitory effect on hind paw swelling. CD68 is an established macrophages' marker, which is up-regulated during the activation of macrophages [27]. Our present data showed that XI could suppress the increased CD68 expression induced by CFA in the ankle joints, showing that the *anti*-RA effect of XI is likely attributed to its inhibitory effect on the activation of macrophages.

Since XI could inhibit the activation of macrophages and the release of inflammatory mediators that are potentially regulated by TLR4 signaling in CFA-induced paw inflammation, we examined whether XI could suppress bacterial LPS-induced TLR4 activation in RAW264.7 cells. It has been reported that activation of TLR4 signaling affects both innate and adaptive immune responses which are essential for RA initiation and progression [28,29]. Therefore, attenuation of TLR4 signaling cascades might be a therapeutic approach for RA treatment. Our present study found that XI could inhibit the secretion of TLR4-related inflammatory mediators, including cytokines (TNF- α , IL-6, and IL-1 β) and chemokines (MCP-1, MIP-1 α , and Rantes) in LPS-stimulated macrophages. Some studies also reported that activation of TLR4 signaling promoted iNOS and COX-2 expression, thereby triggering the immune responses [30,31]. Our study found that the release of NO and PGE2 was decreased after XI treatment, which was related to the reduction of iNOS and COX-2, respectively. Our results suggested that inhibition of the downstream molecules of the TLR4 signaling pathways, such as TNF- α , IL-6, MCP-1, COX-2 and iNOS, may be a part of the mechanisms of anti-inflammatory action of XI.

Next, the key components involving in TLR4 signaling were further investigated. After LPS binding to TLR4, Akt becomes activated by phosphorylation and promotes the phosphorylation of IKK complex (IKK α , IKK β and IKK γ), which is the core element of the NF- κ B cascade [32]. The activated IKK complex then catalyzes the phosphorylation of I κ B, leading to its degradation via ubiquitylation [33]. The removal of I κ B promotes the phosphorylation of NF- κ B and its translocation into the nucleus, initiating the transcription of NF- κ B-dependent inflammatory genes [34]. Our results showed that the phosphorylation IKK α / β and I κ B α was obviously increased after LPS stimulation, and XI treatment lowered the expression of these two proteins. Meanwhile, XI was found to be able to inhibit the phosphorylation and nuclear translocation of NF- κ B. Besides, MAPK/c-Jun signaling pathway is another important component of TLR4, which regulates the production of inflammatory mediators and involves in inflammation and tissue destruction in RA [35,36]. Our data showed that after LPS exposure, XI treatment reduced the activation of phosphorylated MAPKs (p38, ERK, and JNK) and c-Jun. The nuclear translocation of c-Jun was also hindered by XI treatment. In addition, activation of TLR4 signaling leads to the activation of TBK1 which then promotes the nuclear translocation of IRF3 [37]. This triggers the up-regulation of the expression of its target genes (e.g. Rantes) [38]. In our study, we found that XI treatment significantly suppressed the phosphorylation of TBK1 and IRF3 in LPS-exposed RAW264.7 macrophages. We also observed that the nuclear translocation of IRF3 was hindered by XI treatment, revealing that XI treatment inhibited the TBK1/IRF3 signaling transduction. These results demonstrated that XI treatment suppressed the release of cytokines and chemokines via inhibiting various TLR4 signaling components.

Our present study has two limitations. Firstly, application of UPLC-MS analysis might help to further identify other bioactive compounds in addition to chlorogenic acid and rutin in XI. Secondly, as macrophage-mediated overactive inflammatory responses have been implicated in the pathogenesis of RA, we only used LPS-challenged RAW264.7 macrophages to investigate the anti-

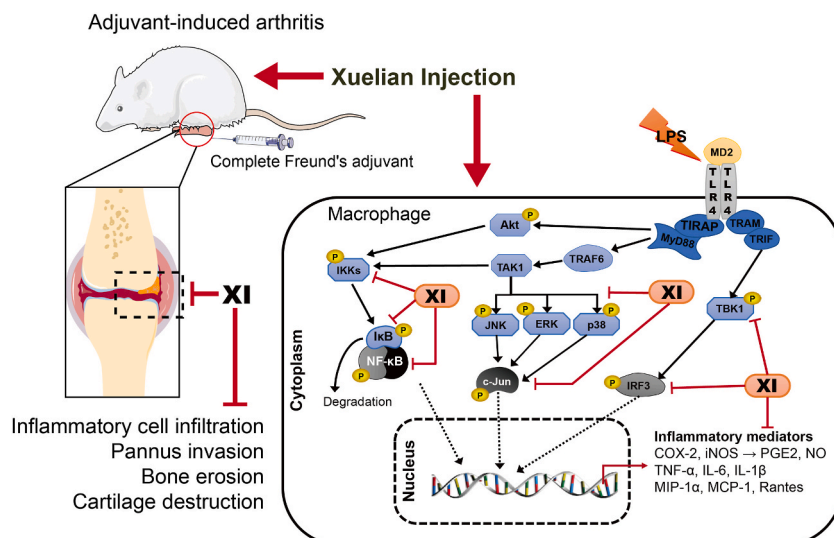


Fig. 7. A schematic diagram showing the association between the inhibition of TLR4 signaling and *anti*-RA effects of XI. XI treatment improved the arthritic parameters of AA rats through the inhibition of macrophage recruitment and TLR4 signaling. XI treatment also suppressed the secretion of inflammatory mediators in LPS-primed RAW264.7 macrophages, which is closely related to its suppressive effect on TLR4 signaling. This figure was partly generated using Servier Medical Art, provided by Servier, licensed under a Creative Commons Attribution 3.0 unported license.

inflammatory effect of XI. In our future study, we will use fibroblast-like synoviocytes, such as MH7A cells, to investigate the suppressive effect of XI on hyperplasia of synovial cells.

5. Conclusions

In conclusion, XI treatment improved the arthritic conditions of AA rats without obvious adverse effects, which was closely related to the suppression of the activation of macrophages and TLR4 signaling. Moreover, XI treatment inhibited the release of inflammatory mediators in LPS-primed RAW264.7 macrophages. The underlying molecular mechanism of this action is related to its suppressive effect on TLR4 signaling (Fig. 7). Our study provide further pharmacological basis for the clinical application of XI in the management of RA.

Funding statement

This work was supported by Fundamental Research Funds for the Central Universities (2018-JYBZZ-XJSJJ008).

Data availability statement

The data associated with the study has not been deposited into a publicly available repository. Data will be made available from the corresponding author upon reasonable request.

CRedit authorship contribution statement

Li-Shan Yan: Data curation, Formal analysis, Investigation, Validation, Visualization, Writing – original draft, Writing – review & editing. **Brian Chi-Yan Cheng:** Writing – original draft, Writing – review & editing. **Yi-Wei Wang:** Data curation, Formal analysis, Investigation. **Shuo-Feng Zhang:** Investigation. **Xin-Yu Qiu:** Investigation. **Jian-Ying Kang:** Investigation. **Chao Zhang:** Investigation. **Zhan-Hong Jia:** Investigation. **Gan Luo:** Formal analysis, Funding acquisition, Investigation, Methodology, Visualization, Writing – review & editing. **Yi Zhang:** Conceptualization, Data curation, Formal analysis, Investigation, Methodology, Project administration, Supervision, Validation, Writing – original draft, Writing – review & editing, Resources.

Declaration of competing interest

The authors declare that they have no known competing financial interests or personal relationships that could have appeared to influence the work reported in this paper.

Appendix A. Supplementary data

Supplementary data to this article can be found online at <https://doi.org/10.1016/j.heliyon.2023.e21635>.

References

- [1] J.S. Smolen, D. Aletaha, I.B. McInnes, Rheumatoid arthritis, *Lancet* 388 (10055) (2016) 2023–2038.
- [2] K. Almutairi, J. Nossent, D. Preen, H. Keen, C. Inderjeeth, The global prevalence of rheumatoid arthritis: a meta-analysis based on a systematic review, *Rheumatol. Int.* 41 (5) (2021) 863–877.
- [3] P.H. Hsieh, O. Wu, C. Geue, E. McIntosh, I.B. McInnes, S. Siebert, Economic burden of rheumatoid arthritis: a systematic review of literature in biologic era, *Ann. Rheum. Dis.* 79 (6) (2020) 771–777.
- [4] J.A. Sparks, Rheumatoid arthritis, *Ann. Intern. Med.* 170 (1) (2019). Itc1-itc16.
- [5] H. Wang, D. Wu, H. Xiang, A. Chen, J. Liu, Pulmonary non-Hodgkin's lymphoma developed during long-term methotrexate therapy for rheumatoid arthritis, *Rheumatol. Int.* 32 (11) (2012) 3639–3642.
- [6] D. Huscher, K. Thiele, E. Gromnica-Ihle, G. Hein, W. Demary, R. Dreher, A. Zink, F. Buttgerit, Dose-related patterns of glucocorticoid-induced side effects, *Ann. Rheum. Dis.* 68 (7) (2009) 1119–1124.
- [7] E. Siouti, E. Andreaskos, The many facets of macrophages in rheumatoid arthritis, *Biochem. Pharmacol.* 165 (2019) 152–169.
- [8] A.K. Rana, Y. Li, Q. Dang, F. Yang, Monocytes in rheumatoid arthritis: circulating precursors of macrophages and osteoclasts and, their heterogeneity and plasticity role in RA pathogenesis, *Int. Immunopharm.* 65 (2018) 348–359.
- [9] Q. Huang, Y. Ma, A. Adebayo, R.M. Pope, Increased macrophage activation mediated through toll-like receptors in rheumatoid arthritis, *Arthritis Rheum.* 56 (7) (2007) 2192–2201.
- [10] Q.Q. Huang, R.M. Pope, The role of toll-like receptors in rheumatoid arthritis, *Curr. Rheumatol. Rep.* 11 (5) (2009) 357–364.
- [11] S.Y. Park, S.W. Lee, S.H. Baek, C.W. Lee, W.S. Lee, Rhim By, K.W. Hong, C.D. Kim, Suppression of PU.1-linked TLR4 expression by cilostazol with decrease of cytokine production in macrophages from patients with rheumatoid arthritis, *Br. J. Pharmacol.* 168 (6) (2013) 1401–1411.
- [12] W.I. Chik, L. Zhu, L.L. Fan, T. Yi, G.Y. Zhu, X.J. Gou, Y.N. Tang, J. Xu, W.P. Yeung, Z.Z. Zhao, et al., *Saussurea involucrata*: a review of the botany, phytochemistry and ethnopharmacology of a rare traditional herbal medicine, *J. Ethnopharmacol.* 172 (2015) 44–60.
- [13] J. Sun, Y. Zhu, L. Zhang, Y. Ma, Effects of xuelian injection on cerebral TNF- α , IL-1 β and MMP-9 in rats experienced focal cerebral ischemia/reperfusion, *Int. J. Clin. Exp. Med.* 7 (9) (2014) 2632–2638.

- [14] S. Hayer, M.J. Vervoordeldonk, M.C. Denis, M. Armaka, M. Hoffmann, J. Bäcklund, K.S. Nandakumar, B. Niederreiter, C. Geka, A. Fischer, et al., 'SMASH' recommendations for standardised microscopic arthritis scoring of histological sections from inflammatory arthritis animal models, *Ann. Rheum. Dis.* 80 (6) (2021) 714–726.
- [15] G. Luo, B.C. Cheng, H. Zhao, X.Q. Fu, R. Xie, S.F. Zhang, S.Y. Pan, Y. Zhang, *Schisandra chinensis* lignans suppresses the production of inflammatory mediators regulated by NF- κ B, AP-1, and IRF3 in lipopolysaccharide-stimulated RAW264.7 cells, *Molecules* 23 (12) (2018).
- [16] D.A. Chistiakov, M.C. Killingsworth, V.A. Myasoedova, A.N. Orekhov, Y.V. Bobryshev, CD68/macrosialin: not just a histochemical marker, *Lab. Invest.* 97 (1) (2017) 4–13.
- [17] J. MacMicking, Q.W. Xie, C. Nathan, Nitric oxide and macrophage function, *Annu. Rev. Immunol.* 15 (1997) 323–350.
- [18] J. Akaogi, T. Nozaki, M. Satoh, H. Yamada, Role of PGE2 and EP receptors in the pathogenesis of rheumatoid arthritis and as a novel therapeutic strategy, *Endocr., Metab. Immune Disord.: Drug Targets* 6 (4) (2006) 383–394.
- [19] K. Takeda, S. Akira, TLR signaling pathways, *Semin. Immunol.* 16 (1) (2004) 3–9.
- [20] X. Fu, X. Lyu, H. Liu, D. Zhong, Z. Xu, F. He, G. Huang, Chlorogenic acid inhibits BAFF expression in collagen-induced arthritis and human synovocyte MH7A cells by modulating the activation of the NF- κ B signaling pathway, *J. Immunol Res* 2019 (2019), 8042097.
- [21] P.S. Chauhan, N.K. Satti, P. Sharma, V.K. Sharma, K.A. Suri, S. Bani, Differential effects of chlorogenic acid on various immunological parameters relevant to rheumatoid arthritis, *Phytother. Res.* 26 (8) (2012) 1156–1165.
- [22] A. Gul, B. Kunwar, M. Mazhar, S. Faizi, D. Ahmed, M.R. Shah, S.U. Simjee, Rutin and rutin-conjugated gold nanoparticles ameliorate collagen-induced arthritis in rats through inhibition of NF- κ B and iNOS activation, *Int. Immunopharm.* 59 (2018) 310–317.
- [23] C.L. Sun, J. Wei, L.Q. Bi, Rutin attenuates oxidative stress and proinflammatory cytokine level in adjuvant induced rheumatoid arthritis via inhibition of NF- κ B, *Pharmacology* 100 (1–2) (2017) 40–49.
- [24] Z. Szekanecz, A.E. Koch, Macrophages and their products in rheumatoid arthritis, *Curr. Opin. Rheumatol.* 19 (3) (2007) 289–295.
- [25] I.B. McInnes, G. Schett, Cytokines in the pathogenesis of rheumatoid arthritis, *Nat. Rev. Immunol.* 7 (6) (2007) 429–442.
- [26] I.B. McInnes, G. Schett, Pathogenetic insights from the treatment of rheumatoid arthritis, *Lancet* 389 (10086) (2017) 2328–2337.
- [27] U. Klinge, A. Dievernich, R. Tolba, B. Klosterhalfen, L. Davies, CD68+ macrophages as crucial components of the foreign body reaction demonstrate an unconventional pattern of functional markers quantified by analysis with double fluorescence staining, *J. Biomed. Mater. Res. B Appl. Biomater.* 108 (8) (2020) 3134–3146.
- [28] M.F. Roelofs, W.C. Boelens, L.A. Joosten, S. Abdollahi-Roodsaz, J. Geurts, L.U. Wunderink, B.W. Schreurs, W.B. van den Berg, T.R. Radstake, Identification of small heat shock protein B8 (HSP22) as a novel TLR4 ligand and potential involvement in the pathogenesis of rheumatoid arthritis, *J. Immunol.* 176 (11) (2006) 7021–7027.
- [29] M.I. Edilova, A. Akram, A.A. Abdul-Sater, Innate immunity drives pathogenesis of rheumatoid arthritis, *Biomed. J.* 44 (2) (2021) 172–182.
- [30] M. Hori, M. Kita, S. Torihashi, S. Miyamoto, K.J. Won, K. Sato, H. Ozaki, H. Karaki, Upregulation of iNOS by COX-2 in muscularis resident macrophage of rat intestine stimulated with LPS, *Am. J. Physiol. Gastrointest. Liver Physiol.* 280 (5) (2001) G930–G938.
- [31] Y. Zhu, M. Zhu, P. Lance, iNOS signaling interacts with COX-2 pathway in colonic fibroblasts, *Exp. Cell Res.* 318 (16) (2012) 2116–2127.
- [32] T. Liu, L. Zhang, D. Joo, S.C. Sun, NF- κ B signaling in inflammation, *Signal Transduct. Targeted Ther.* 2 (2017), 17023.
- [33] T. Lawrence, The nuclear factor NF- κ B pathway in inflammation, *Cold Spring Harbor Perspect. Biol.* 1 (6) (2009), a001651.
- [34] K. Taniguchi, M. Karin, NF- κ B, inflammation, immunity and cancer: coming of age, *Nat. Rev. Immunol.* 18 (5) (2018) 309–324.
- [35] Z. Han, D.L. Boyle, L. Chang, B. Bennett, M. Karin, L. Yang, A.M. Manning, G.S. Firestein, c-Jun N-terminal kinase is required for metalloproteinase expression and joint destruction in inflammatory arthritis, *J. Clin. Invest.* 108 (1) (2001) 73–81.
- [36] G. Schett, M. Tohidast-Akrad, J.S. Smolen, B.J. Schmid, C.W. Steiner, P. Bitzan, P. Zenz, K. Redlich, Q. Xu, G. Steiner, Activation, differential localization, and regulation of the stress-activated protein kinases, extracellular signal-regulated kinase, c-JUN N-terminal kinase, and p38 mitogen-activated protein kinase, in synovial tissue and cells in rheumatoid arthritis, *Arthritis Rheum.* 43 (11) (2000) 2501–2512.
- [37] K.A. Fitzgerald, S.M. McWhirter, K.L. Faia, D.C. Rowe, E. Latz, D.T. Golenbock, A.J. Coyle, S.M. Liao, T. Maniatis, IKKepsilon and TBK1 are essential components of the IRF3 signaling pathway, *Nat. Immunol.* 4 (5) (2003) 491–496.
- [38] S.M. McWhirter, K.A. Fitzgerald, J. Rosains, D.C. Rowe, D.T. Golenbock, T. Maniatis, IFN-regulatory factor 3-dependent gene expression is defective in Tbk1-deficient mouse embryonic fibroblasts, *Proc. Natl. Acad. Sci. U.S.A.* 101 (1) (2004) 233–238.